Constraints on Parton Charge Symmetry and Implications for Neutrino Reactions

J.T.Londergan*
Department of Physics and Nuclear Theory Center, Indiana University, Bloomington, IN 47405, USA

A.W.Thomas†
Jefferson Lab, 12000 Jefferson Ave., Newport News, VA 23606, USA

(Dated: February 2, 2008)

For the first time, charge symmetry breaking terms in parton distribution functions have been included in a global fit to high energy data. We review the results obtained for both valence and sea quark charge symmetry violation, and we compare these results with the most stringent experimental upper limits on charge symmetry violation for parton distribution functions, and with theoretical estimates of charge symmetry violation. The limits allowed in the global fit would tolerate a rather large violation of charge symmetry. We discuss the implications of this for the extraction of the Weinberg angle in neutrino DIS by the NuTeV collaboration.

PACS numbers: 11.30.Hv, 12.15.Mm, 12.38.Qk, 13.15.+g

I. INTRODUCTION

Charge symmetry is a restricted form of isospin invariance involving a rotation of 180° about the "2" axis in isospin space. For parton distributions, charge symmetry involves interchanging up and down quarks while simultaneously interchanging protons and neutrons. In nuclear physics, charge symmetry is generally obeyed at the level of a fraction of a percent [1, 2]. Charge symmetry violation in parton distribution functions (PDFs) arises from two sources; from the difference $\delta m \equiv m_d - m_u$ between down and up current quark masses, and from electromagnetic (EM) effects.

Since charge symmetry is so well satisfied at lower energies, it is natural to assume that it holds for parton distributions. Introducing charge symmetry reduces by a factor of two the number of PDFs necessary to describe high-energy data. In addition, as we shall see, there is no direct experimental evidence that points to a substantial violation of charge symmetry in parton distributions. For this reason, until recently all phenomenological PDFs have assumed charge symmetry at the outset. In Sec. II, we review the experimental evidence for charge symmetry in PDFs. Recent experiments allow us to place reasonably strong upper limits on parton charge symmetry violation. In Sec. III, we review some theoretical estimates for parton charge symmetry violation (CSV) for valence quarks, and we compare this with the experimental limits. In Sec. IV, we review the recent global fit by Martin *et al.,* [3] that includes for the first time the possibility of charge symmetry violating PDFs both for valence and for sea quarks. We compare the results of this phenomenological fit with the experimental limits on parton CSV as well as with theoretical estimates of both the magnitude and sign of charge symmetry violating parton distributions.

In Sect. V, we review the effect of isospin violating PDFs on neutrino DIS measurements. In particular, we concentrate on the extraction of the Weinberg angle by the NuTeV collaboration [4]. We show the magnitude of the effects predicted by theoretical calculations, and we contrast this with the magnitude of effects allowed by the phenomenological CSV PDFs extracted by the MRST group [3].

II. EXPERIMENTAL LIMITS ON PARTON CHARGE SYMMETRY VIOLATION

There are no direct measurements that reveal the presence of charge symmetry violation in parton distribution functions. At present, we have only upper limits on the magnitude of charge symmetry violation.

The most stringent test of parton charge symmetry comes from comparing the structure function F_2^ν measured in neutrino induced charged current reactions, and the structure function F_2^γ for charged lepton DIS, both measured on isoscalar targets N_0. In leading order, assuming parton charge symmetry, the structure functions have the form [5]

$$\begin{aligned} F_2^{\gamma N_0}(x) &\approx \frac{5Q(x)}{18} + \frac{x}{6}\left(c(x)+\bar{c}(x)-s(x)-\bar{s}(x)\right) \\ F_2^{W^\pm N_0}(x) &\approx Q(x) \pm x\left(s(x)-\bar{s}(x)+\bar{c}(x)-c(x)\right) \\ Q(x) &= \sum_{j=u,d,s,c} x\left(q_j(x)+\bar{q}_j(x)\right) \end{aligned} \quad (1)$$

In Eq. 1, $F_2^{W^\pm N_0}$ is the structure function for charged-current processes induced by neutrinos (antineutrinos)

*Electronic address: tlonderg@indiana.edu
†Electronic address: awthomas@jlab.org

on an isoscalar target. Charge symmetry violation and NLO effects are not included in this equation. In the limit of exact charge symmetry, there is a simple relation between the charged-lepton and neutrino structure functions, corrected for heavy quark effects. This relation is defined as the "charge ratio" $R_c(x,Q^2)$ or, as it is sometimes termed, the "$5/18^{th}$ rule." The factor 5/18 is simply understood as the average of the squares of the light quark charges, relative to the weak charges. Expanding R_c to lowest order in the (presumably small) charge symmetry violating terms gives

$$R_c(x) \equiv \frac{F_2^{\gamma N_0}(x) + x\left(s(x)+\bar{s}(x)-c(x)-\bar{c}(x)\right)/6}{5\overline{F_2}^{WN_0}(x)/18} \approx 1 + \frac{3x\left(\delta u(x)+\delta\bar{u}(x)-\delta d(x)-\delta\bar{d}(x)\right)}{10\,Q(x)} \quad (2)$$

Eq. 2 introduces the CSV parton distributions,

$$\delta u(x) = u^p(x) - d^n(x)\,; \qquad \delta d(x) = d^p(x) - u^n(x)\,, \quad (3)$$

with analogous relations for antiquarks. The quantity $R_c(x)$ in Eq. 2 is defined using $\overline{F_2}^{WN_0}$, the average of neutrino and antineutrino, F_2, charge-changing structure functions; it also requires knowledge of strange and charm PDFs. Deviation of $R_c(x)$ from unity would be an indication of a non-zero charge symmetry violating contribution.

The most precise neutrino measurements were obtained by the CCFR group [6], who extracted the F_2 structure function for neutrino and antineutrino interactions on iron using the Quadrupole Triplet Beam at FNAL. This can be compared with several measurements of the F_2 structure functions from DIS reactions using high-energy muons or electrons. The most precise measurements were obtained by the NMC group [7, 8], who measured F_2 structure functions for muon interactions on deuterium at muon energies $E_\mu = 90$ and 280 GeV. Earlier measurements were obtained by the BCDMS muon scattering experiments on deuterium [9] and carbon [10], and electron scattering results from SLAC [11, 12].

Precision measurements of the charge ratio require a significant number of corrections. It is necessary to know the relative normalization between charged-lepton and neutrino cross sections. Heavy quark threshold effects are very important, as the most important neutrino energies are sufficiently small that one must correct for the finite mass of the charmed quark [13]. The CCFR neutrino cross sections were taken on iron targets, so one must correct for nuclear effects (Fermi motion at large x, EMC effects at intermediate x and shadowing at small x [14, 15, 16, 17, 18, 19]). There are additional corrections since iron is not an isoscalar target. Eq. 2 also requires contributions from strange and charmed quarks. The CCFR [20] and NuTeV [21] groups have extracted strange (antistrange) quark distributions from the cross sections for opposite sign dimuons in reactions induced by neutrinos (antineutrinos).

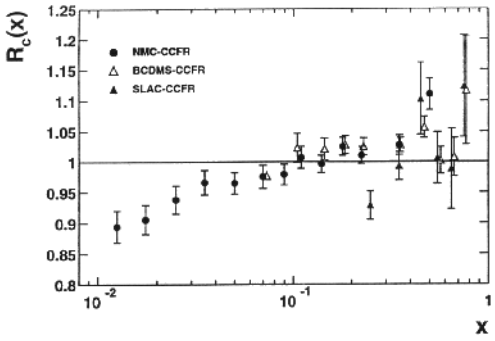

FIG. 1: The charge ratio of Eq. 2 vs. x using CCFR neutrino data of Ref. [6] combined with muon DIS data. Solid circles: NMC $\mu - D$ data, Ref. [7]; open triangles: muon measurements from the BCDMS group on D, Ref. [9] and C, Ref. [10]; solid triangles: SLAC electron scattering data Refs. [11, 12].

Fig. 1 plots the charge ratio R_c of Eq. 2 vs. x. The circles are the NMC/CCFR ratio. The open triangles are the BCDMS/CCFR charge ratio, where BCDMS represents the muon scattering results of the BCDMS group on deuterium [9] and carbon [10]. The solid triangles are the SLAC/CCFR charge ratio, where SLAC denotes electron scattering results of the SLAC group [11, 12]. Since the CCFR measurements were obtained from neutrino-iron scattering, and the NMC measurements were from $\mu - D$ reactions, the NMC measurements were "converted" to the equivalent reactions on iron by multiplying by the ratio of $\mu - Fe$ to $\mu - D$ cross sections [22, 23]. In addition, a correction for strange quarks and charm quarks was applied to the numerator of Eq. 2.

In the region $0.1 \le x \le 0.4$ the charge ratio test is consistent with unity, with errors in the range $2-3\%$. Solving Eq. 2 for the CSV parton distributions,

$$\frac{x\left(\delta u(x)+\delta\bar{u}(x)-\delta d(x)-\delta\bar{d}(x)\right)}{Q(x)} = \frac{10}{3}\left(R_c - 1\right) \quad (4)$$

one can set an upper limit to parton CSV effects in this x range at about the $6-9\%$ level. For larger values of x the upper limit on CSV effects is substantially greater. This is due both to poorer statistics and to the large Fermi motion corrections needed for the heavy target at large x.

At values $x < 0.1$, the charge ratio appeared to deviate significantly from unity. The discrepancy increased monotonically as x decreased, and approached 15% at the smallest values of x [24]. Several suggestions were advanced to explain this discrepancy, including anomalously large contributions from strange quarks [25], and surprisingly large contributions from sea quark charge symmetry violation [26]. Eventually the CCFR group re-

analyzed the neutrino data, and after the new analysis the small-x discrepancy disappeared [27], largely as a result of two factors. The first was the treatment of charm mass corrections. In the initial analysis, these were incorporated using the "slow rescaling" hypothesis due to Georgi and Politzer [28]. The re-analysis involved NLO calculations, which differed significantly from the slow-rescaling procedure at small x – as had been suggested by Boros *et al.* [29]. Since the NLO effects depend on both x and Q^2, the final results cannot be plotted simply versus Bjorken x.

The second significant effect involved the separation of the F_2 and F_3 structure functions in charged-current neutrino DIS. The sum of neutrino and antineutrino charged-current DIS cross sections contains a linear combination of neutrino F_2 and F_3 structure functions,

$$\frac{d^2\sigma^{\nu}_{CC}}{dxdy} + \frac{d^2\sigma^{\bar{\nu}}_{CC}}{dxdy} \sim 2(1-y-y^2/2)\overline{F}_2(x,Q^2) + (y-y^2/2)\Delta xF_3(x,Q^2)\,. \quad (5)$$

In Eq. 5, $\overline{F}_2$ is the average of the F_2 structure functions for neutrinos and antineutrinos, and in leading order (assuming charge symmetry), $\Delta xF_3 = 2x(s+\bar{s}-c-\bar{c})$. The structure functions are multiplied by coefficients that depend on the invariant $y = p\cdot q/p\cdot k$, where $k(p)$ is the four momentum of the initial lepton (nucleon), and q is the four momentum of the virtual W exchanged in the interaction. In Eq. 5 we have dropped terms of order m_N^2/s, and for simplicity the longitudinal/transverse ratio R has been set to zero.

In the initial data analysis, the data for a given x bin was averaged over all y, and the ΔxF_3 structure function was estimated using phenomenological PDFs. The re-analysis included the x, y and Q^2 dependence of the cross sections. In this way the group was able to extract both $\overline{F}_2$ and ΔxF_3. The experimental values for ΔxF_3 differed substantially from the phenomenological predictions. This affected the extracted values for the F_2 neutrino structure functions. The description of charm production also plays a significant role in determining the value of ΔxF_3 [30, 31, 32]. The combined effect of the NLO treatment of charm production, and the model-independent extraction of ΔxF_3 removed the small-x discrepancy. The charge ratio R_c of Eq. 2 is now unity to within experimental errors, even at small x. Since the NLO treatment depends separately on Q^2 and x, it is no longer possible to display the results in a Q^2-independent plot such as Fig. 1.

III. THEORETICAL ESTIMATES OF PARTON CHARGE SYMMETRY VIOLATION

Both the quark mass difference and EM effects responsible for parton charge symmetry violation represent small changes to quark PDFs. Several theoretical estimates of parton CSV for valence quarks can be obtained by examining simple models for parton distribution functions, then observing how these change upon applying the operations of charge symmetry.

The Adelaide group [5, 33, 34, 35] developed a method for calculating twist-two valence parton distributions through the relation

$$q_{\rm v}(x,\mu^2) = M\sum_X |\langle X|\psi_+(0)|N\rangle|^2\delta(M(1-x)-p_X^+)\,. \quad (6)$$

In Eq. 6, $\psi_+ = (1+\alpha_3)\psi/2$ is the operator that removes a quark or adds an antiquark to the nucleon state $|N\rangle$, μ^2 is the starting scale (where QCD is best approximated by a valence dominated quark model) for the quark distribution, $|X\rangle$ represents all possible final states that can be reached with this operator (*i.e.,* $|X\rangle = 2q, 3q+\overline{q}, 4q+2\overline{q}, \ldots$), and p_X^+ is the plus component ($p^+ \equiv p_3 + E(p)$) of the momentum of the residual system. We note that the advantage of using Eq. 6 is that the correct support for the PDF is assured, regardless of the approximation used to evaluate the nonperturbative matrix element $\langle X|\psi_+(0)|N\rangle$.

Sather [36] assumed that the dominant result of electromagnetic effects was manifested in the neutron-proton mass difference $\delta M \equiv M_n - M_p$. At the low Q^2 appropriate to quark models, the largest contribution to valence PDFs at large x arises from configurations where one quark is removed from three valence quarks, leaving a residual diquark. Since CSV corresponds to interchanging up and down quark, and neutron-proton labels, valence quark CSV is obtained by examining how Eq. 6 changes with δm and δM.

Restricting Eq. 6 to the residual diquark state $X = 2$ (valid for large x) and neglecting the dependence on transverse momentum in the δ-function, Sather obtained analytic relations between valence quark CSV and derivatives of the valence PDFs,

$$\begin{aligned}
\delta d_{\rm v}(x) &\equiv d^p_{\rm v}(x) - u^n_{\rm v}(x) \\
&= -\frac{\delta M}{M}\frac{d}{dx}\left[x d_{\rm v}(x)\right] - \frac{\delta m}{M}\frac{d}{dx}d_{\rm v}(x) \\
\delta u_{\rm v}(x) &\equiv u^p_{\rm v}(x) - d^n_{\rm v}(x) \\
&= \frac{\delta M}{M}\left(-\frac{d}{dx}\left[x u_{\rm v}(x)\right] + \frac{d}{dx}u_{\rm v}(x)\right) \quad (7)
\end{aligned}$$

In Eq. (7), M is the average nucleon mass, $\delta M = 1.3$ MeV is the n-p mass difference, and $\delta m = m_d - m_u \sim 4$ MeV is the down-up quark mass difference. From Eq. 7, at large x the down quark valence distribution in the proton is expected to be larger than the up quark distribution in the neutron; similarly, the down quark distribution in the neutron is larger than the up quark distribution in the proton at large x. The lowest moment of the valence quark distributions is fixed by quark normalization, since

$$\int_0^1 dx\delta d_{\rm v}(x) = \int_0^1 dx\delta u_{\rm v}(x) = 0\,. \quad (8)$$

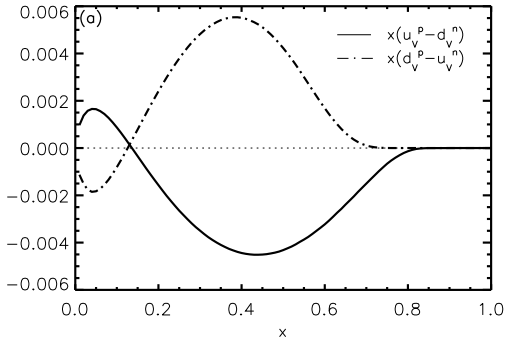

FIG. 2: Valence quark CSV contributions, $x\delta q_{\rm v}(x)$ vs. x. Solid line: $x\delta u_{\rm v}$; dash-dot line: $x\delta d_{\rm v}$. Calculated by Rodionov *et al.,* Ref. [37] using MIT bag model wavefunctions, evolved to $Q^2 = 10$ GeV^2.

A violation of Eq. 8 would be equivalent to changing the total number of valence quarks in the proton and/or neutron. Eq. 8 shows that if $\delta d_{\rm v}(x)$ is positive at large x, it must therefore be negative at small x such that the integral over all x vanishes; similarly, the quantity $\delta u_{\rm v}(x)$ must also change sign at small x.

Sather's results do not include effects from configurations with more than two quarks in the final state. In addition, his analytic results include only the contribution from quark longitudinal momentum (effects from quark transverse momentum in Eq. 6 are neglected). Rodionov *et al.,* [37] explicitly included the effect quark transverse momentum within the MIT bag model. They did not use the approximate equations of Sather, but included quark and nucleon mass differences directly in Eq. 6. Their results for valence quark CSV PDFs are shown in Fig. 2. The solid curve is $x\delta u_{\rm v}(x)$, while the dot-dashed curve is $x\delta d_{\rm v}(x)$, both evolved to $Q^2 = 10$ GeV^2. Qualitatively, the results of Rodionov *et al.* are very similar to Sather's. The sign and relative magnitude of both $\delta d_{\rm v}(x)$ and $\delta u_{\rm v}(x)$ are quite similar in both calculations, and the second moment of both distributions is equal to better than 10%.

IV. PHENOMENOLOGICAL CHARGE SYMMETRY VIOLATING PDFS

Because CSV effects are typically very small at nuclear physics energy scales [1, 2], from the lack of direct evidence for violation of parton charge symmetry, and because theoretical estimates put parton CSV at below the 1% level [5], all previous phenomenological parton distribution functions have assumed the validity of parton charge symmetry at the outset. However, Martin, Roberts, Stirling and Thorne (MRST) [3] have recently studied the uncertainties in parton distributions arising from a number of factors, including isospin violation.

The MRST group chose a specific model for valence quark charge symmetry violating PDFs. They constructed a function that automatically satisfied the quark normalization condition of Eq. 8, namely:

$$\begin{aligned} \delta u_{\rm v}(x) &= -\delta d_{\rm v}(x) = \kappa f(x) \\ f(x) &= (1-x)^4 x^{-0.5}\,(x - .0909)\,. \end{aligned} \tag{9}$$

The function $f(x)$ was chosen so that at both small and large x, $f(x)$ has the same form as the MRST valence quark distributions, and the first moment of $f(x)$ is zero. The functional form of the valence CSV distributions guaranteed that $\delta u_{\rm v}$ and $\delta d_{\rm v}$ would have opposite signs at large x, in agreement with the theoretical results shown in Fig. 2.

Inclusion of a valence quark CSV term changes the up and down quark distributions in the neutron from their charge symmetric counterparts in the proton. This changes the momentum carried by valence quarks in the neutron from those in the proton, since the total momentum carried by valence quarks is given by the second moment of the distribution, *e.g.,* the momentum carried by up valence quarks in the neutron

$$U_{\rm v}^n \equiv \int_0^1 x\, u_{\rm v}^n(x)\, dx\ .$$

Because the total momentum carried by valence (up plus down) quarks in the neutron, $U_{\rm v}^n + D_{\rm v}^n$, is rather precisely determined, MRST chose a functional form that kept this quantity relatively constant. For this reason, they insisted that the valence CSV terms for up and down quarks in the nucleon be equal and opposite. Note that QCD evolution does not preserve this relation, but it is very nearly maintained for the region of evolution of interest. The overall coefficient, κ, was then varied in a global fit to a wide range of high energy data.

The value of κ which minimised χ^2 was $\kappa = -0.2$. The MRST χ^2 vs. κ is shown as the bottom curve in Fig. 3. Clearly χ^2 has a shallow minimum with the 90% confidence level obtained for the range $-0.8 \leq \kappa \leq +0.65$. Since the form chosen by MRST for valence quark CSV is strongly constrained, and the resulting χ^2 minimum is quite shallow, one should not assign too much significance to their result. In global fits of this type, one should remember that, unless the shape of the constrained function is in close agreement with the actual parton distribution, the overall magnitude obtained in a global fit can be misleading. In Fig. 4 we plot the valence quark CSV PDFs corresponding to the MRST best fit value $\kappa = -0.2$. They look extremely similar to the theoretical valence quark PDFs calculated by Rodionov *et al.* and shown in Fig. 2; they are also in good agreement with Sather's valence CSV distributions. This provides some theoretical support for the functional form chosen

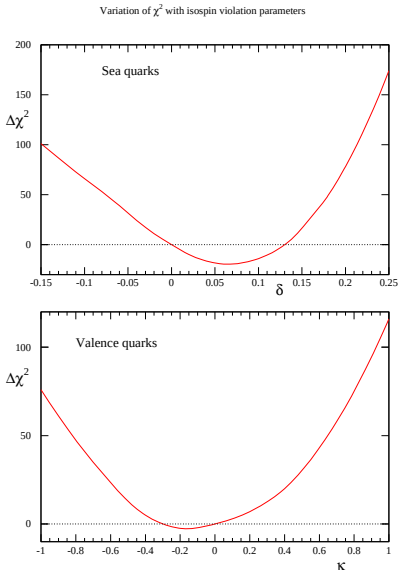

FIG. 3: χ^2 profile for phenomenological isospin violating parton distributions, for sea quarks (top curve) and valence quarks (bottom curve), from the MRST group, Ref. [3]. The quantity δ associated with sea quark isospin violation is defined in Eq. 10, while the coefficient κ is defined in Eq. 9.

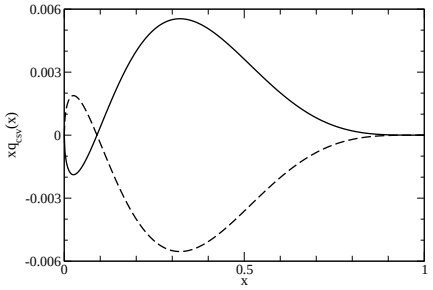

FIG. 4: The valence quark CSV function from Ref. [3], corresponding to best fit value $\kappa = -0.2$ defined in Eq. 9. Solid curve: $x\delta d_v(x)$; dashed curve: $x\delta u_v(x)$.

by MRST. However, within the 90% confidence region for the global fit, the valence quark CSV PDFs could be either four times as large as that predicted by Sather or Rodionov, or it could be three times as big with the opposite sign. The great value of the MRST global fit is that CSV distributions with this shape, and with values of κ within this range, will not disagree seriously with any of the high energy data used to extract quark and gluon distribution functions.

The MRST group also searched for the presence of charge symmetry violation in the sea quark sector. Again, they chose a specific form for sea quark CSV, dependent on a single parameter, *i.e.,*

$$\begin{aligned} \bar{u}^n(x) &= \bar{d}^p(x)\,[1+\delta] \\ \bar{d}^n(x) &= \bar{u}^p(x)\,[1-\delta] \end{aligned} \qquad (10)$$

With the form chosen, the net momentum carried by antiquarks is approximately conserved; violation of momentum conservation was found to be very small in the kinematic region of interest.

Somewhat surprisingly, evidence for sea quark CSV in the global fit is substantially stronger than that for valence quark CSV. As shown in the top curve in Fig. 3, the best fit is obtained for $\delta = 0.08$, corresponding to an 8% violation of charge symmetry in the nucleon sea. The χ^2 corresponding to this value is substantially better than with no charge symmetry violation, primarily because of the improvement in the fit to the NMC $\mu - D$ DIS data [7, 8] when $\bar{u}^n$ is increased. The fit to the E605 Drell-Yan data [38] is also substantially improved by the sea quark CSV term.

We can check the MRST results by comparing them with the charge ratio measurements that were summarized in Sect. II. Eq. 4 relates the CSV parton distributions to the charge ratio through

$$R_c - 1 \;=\; \frac{3x}{10Q(x)}\left(\delta u(x) + \delta\bar{u}(x) - \delta d(x) - \delta\bar{d}(x)\right) .$$

We have taken the valence and sea quark PDFs from MRST [39], and in Fig. 5 we plot them against the experimental charge ratio obtained using the CCFR charged-current neutrino structure function and the NMC muon structure function. The long-dashed curve corresponds to the sea quark CSV term with the best value $\delta = 0.08$ from the MRST fit. The remaining curves correspond to various values for valence quark CSV. The solid curve corresponds to the best value $\kappa = -0.2$, the short-dashed curve corresponds to $\kappa = -0.8$, and the dash-dot curve corresponds to $\kappa = +0.65$. The latter two correspond to values of κ at the 90% confidence level for the MRST fit to valence quark CSV. For values $x < 0.085$, we have not included the charge ratio experimental data since these changed significantly in the CCFR re-analysis. However, the re-analyzed data resulted in a charge ratio that agreed with unity at about the 2-3% level, even down to $x \approx 0.01$.

Both the valence and sea quark CSV distributions of MRST are in good agreement with the experimental limits from the CCFR/NMC data. At every x value the phenomenological values are within two standard deviations of the data. This is understandable, since both the NMC and CCFR data were included in the MRST global fit that extracted the CSV parameters. We have not included overall normalization errors, of roughly 2%, on both the CCFR and NMC data. Since the best fit valence quark PDFs of MRST (the solid curve in Fig. 5) are very close to the theoretical predictions of Sather and Rodionov, the theoretical predictions are well within the upper limits on parton CSV from the best experiments. CSV effects in reasonable agreement with high energy data are substantially larger than predicted by theory; valence CSV effects could be four times as large as predicted by Sather or Rodionov (or three times as large with the opposite sign), and sea quark CSV effects are

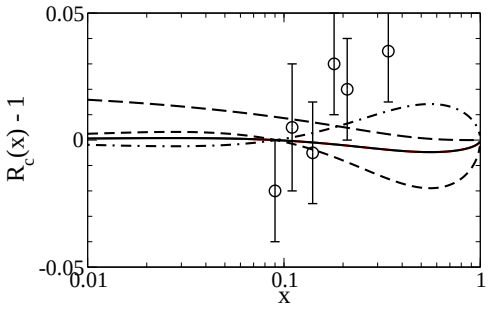

FIG. 5: The "charge ratio" $R_c - 1$ defined in Eq. 2, compared with charge symmetry violating PDFs obtained by the MRST global fit, Ref. [3]. Data is obtained from CCFR neutrino cross sections of Ref. [6] and NMC muon DIS, Ref. [7, 8]. Long-dashed curve: sea quark CSV with best fit parameter $\delta = 0.08$ in Eq. 10; solid curve: valence quark CSV corresponding to best fit value $\kappa = -0.2$ in Eq. 9; short dashed curve: valence quark CSV for $\kappa = -0.8$; dash-dot curve: valence quark CSV for $\kappa = +0.65$.

also significantly larger than theoretical predictions [40].

The only remaining issue is whether the theoretical and phenomenological PDFs agree with the limits on parton momentum, estimated by MRST as relative errors of about 4%. The best value obtained by MRST was $\kappa = -0.2$. With this value, one obtains the relative momentum change for valence neutrons

$$\frac{2|\delta U_{\rm v}|}{U_{\rm v} + D_{\rm v}} = \frac{2\delta D_{\rm v}}{U_{\rm v} + D_{\rm v}} \approx 1\% \qquad (11)$$

This value is well within experimental limits. Even the largest value of κ within the 90% confidence limit, $\kappa = -0.8$, corresponds to a momentum change of 4%. Thus all of the phenomenological valence CSV distributions (and the theoretical distributions of Sather and Rodionov *et al.*) correspond to momentum values within experimental limits.

V. CHARGE SYMMETRY VIOLATION AND NEUTRINO DIS REACTIONS

In 1973, Paschos and Wolfenstein [41] suggested that the ratio of neutral-current and charge-changing neutrino cross sections on isoscalar targets could provide an independent measurement of the Weinberg angle ($\sin^2\theta_W$). The Paschos-Wolfenstein (PW) ratio R^- is given by

$$R^- \equiv \frac{\langle\sigma_{NC}^{\nu N_0}\rangle - \langle\sigma_{NC}^{\overline{\nu} N_0}\rangle}{\rho_0^2\left(\langle\sigma_{CC}^{\nu N_0}\rangle - \langle\sigma_{CC}^{\overline{\nu} N_0}\rangle\right)} = \frac{1}{2} - \sin^2\theta_W. \qquad (12)$$

In Eq. 12, $\langle\sigma_{NC}^{\nu N_0}\rangle$ and $\langle\sigma_{CC}^{\nu N_0}\rangle$ are respectively the neutral-current and charged-current inclusive, total cross sections for neutrinos (or antineutrinos) on an isoscalar target. The quantity $\rho_0 \equiv M_W/(M_Z\cos\theta_W)$ is one in the Standard Model. Not only is the PW ratio independent of parton distribution functions, but in this ratio a large number of partonic corrections either cancel or are minimized.

The NuTeV group has measured neutrino charged-current and neutral-current cross sections on iron [4] and extracted a value for $\sin^2\theta_W$ equal to $0.2277 \pm 0.0013\,(stat) \pm 0.0009\,(syst)$. This value is three standard deviations above the measured fit to other electroweak processes, $\sin^2\theta_W = 0.2227 \pm 0.00037$ [42]. Such an effect can be interpreted as a 1.2% decrease in the left-handed coupling of light valence quarks to the weak neutral current. In addition to the Weinberg angle, several of the parameters of the Standard Model are constrained by the very precise measurements at electron-positron colliders [42]. Indeed, many of these parameters are determined at about the 0.1% level. Consequently, the discrepancy between NuTeV and electromagnetic measurements of the Weinberg angle is surprisingly large. It suggests evidence of physics beyond the Standard Model, although Davidson *et al.,* [43] have shown that it is quite difficult to produce "new physics" (*i.e.,* beyond the Standard Model) that fits the NuTeV experiment without violating other experimental constraints. In this paper, we will examine isospin-violating corrections to the NuTeV experiment.

The NuTeV group did not directly measure the PW ratio, but instead measured the neutral-current to charged-current ratios R^ν and $R^{\overline{\nu}}$. These quantities, and their relation to the PW ratio, are given by

$$\begin{aligned} R^\nu &\equiv \frac{\langle\sigma_{NC}^{\nu N_0}\rangle}{\rho_0^2\langle\sigma_{CC}^{\nu N_0}\rangle}, \qquad R^{\overline{\nu}} \equiv \frac{\langle\sigma_{NC}^{\overline{\nu} N_0}\rangle}{\rho_0^2\langle\sigma_{CC}^{\overline{\nu} N_0}\rangle} \\ R^- &= \frac{\left(R^\nu - R^{\overline{\nu}}\right)}{1 - r\,R^\nu}, \qquad r = \frac{\langle\sigma_{CC}^{\overline{\nu} N_0}\rangle}{\langle\sigma_{CC}^{\nu N_0}\rangle} \end{aligned} \qquad (13)$$

After measuring the ratios R^ν and $R^{\overline{\nu}}$, the NuTeV group obtain the Weinberg angle through a detailed Monte Carlo simulation of the experiment. As a result, it is substantially more difficult to estimate the errors due to corrections to this experiment. For partonic corrections, the NuTeV group [44] have provided functionals that estimate the change in an experimental quantity $\mathcal{E}$ due to changes in a parton distribution $\delta(x)$:

$$\Delta\mathcal{E} \equiv \int_0^1 F\left[\mathcal{E}, \delta; x\right]\,\delta(x)\,dx. \qquad (14)$$

In Eq. 14, $F\left[\mathcal{E}, \delta; x\right]$ is the functional, and the net change in the observable is obtained by integrating over Bjorken x. The NuTeV collaboration provided functionals appropriate for both valence and sea quark CSV.

The correction to the Paschos-Wolfenstein ratio arising from isospin violation in the parton distribution functions has the form

$$\begin{aligned} \Delta R_{CSV} &= \left[1 - \frac{7}{3}\sin^2\theta_W + \frac{4\alpha_s}{9\pi}\left(\frac{1}{2} - \sin^2\theta_W\right)\right] \\ &\cdot\ \frac{\delta U_{\rm v} - \delta D_{\rm v}}{2(U_{\rm v} + D_{\rm v})}, \end{aligned}$$

$$\text{where} \qquad \delta Q_{\rm v} \;=\; \int_0^1 x\,\delta q_{\rm v}(x)\,dx\,. \tag{15}$$

Note that the isospin violating correction to the PW ratio arises entirely from charge symmetry violation in the valence PDFs. Inserting the quark model results of Sather [36] and Rodionov *et al.* [37] into Eq. 15, the CSV correction to the PW ratio is found to be $\Delta R_{CSV} = -0.0021$ using Sather's parton distributions, and $\Delta R_{CSV} = -0.0020$ using the CSV distributions of Rodionov *et al.,* [45]. These are theoretical *predictions*, as the Sather and Rodionov papers were published in 1992 and 1994, respectively, well before the analysis of the NuTeV data. Like the isoscalar corrections to the PW ratio, the CSV corrections involve the ratio of identical moments of parton distributions, and are thus independent of Q^2; consequently they do not depend on any details of QCD evolution.

The negative sign of the result means that CSV corrections will decrease the discrepancy between the NuTeV result for the Weinberg angle, and the Weinberg angle extracted from the extremely precise data obtained from electron-positron colliders near the Z mass. Indeed, the predicted CSV corrections to the PW ratio remove roughly 40% of the magnitude of the NuTeV anomaly. As discussed in the preceding Section, less than 1% of the valence quark momentum is carried by the relevant CSV combination, so this is well within the experimental limits on quark momentum.

Londergan and Thomas [46] showed that Sather's formula of Eq. 7 provided an analytic estimate of CSV corrections to the PW ratio; taking the second moment of Sather's equations gives

$$\delta D_{\rm v} = \frac{\delta M}{M} D_{\rm v} + \frac{\delta m}{M}\,; \qquad \delta U_{\rm v} = \frac{\delta M}{M}\,(U_{\rm v} - 2) \tag{16}$$

Sather's approximation predicts that the CSV correction to the PW ratio depends only on the fraction of nucleon momentum carried by up and down valence quarks. Eq. 16 predicts that $\delta D_{\rm v}$ will be positive and $\delta U_{\rm v}$ negative, in agreement with the theoretical model results. It is especially interesting that Sather's analytic approximation allows one to calculate the CSV correction to the PW ratio directly from valence quark PDFs, without ever having to calculate specific CSV distributions. Using Eq. 16, we also calculated the CSV correction to the PW ratio using the CTEQ4LQ phenomenological parton distribution [47] at $Q^2 = 0.49$ GeV^2, obtaining $\Delta R_{CSV} = -0.0021$ – again in agreement with the results obtained from the two quark model calculations. Eq. 16 shows why the CSV corrections are so similar in various models; the correction depends only on the momentum carried by up and down valence quarks, a quantity well determined in PDFs.

Since the NuTeV group [4, 44] did not directly measure the PW ratio, one must multiply the CSV PDFs with the relevant functional in Eq. 14 [44]. This requires evolving the CSV parton distribution functions from the quark-model scale to $Q^2 = 20$ GeV^2, the average momentum transfer for the NuTeV experiment. After QCD evolution and folding with the NuTeV functionals, the resulting CSV corrections to the NuTeV result are $\Delta R_{CSV} = -0.0015, -.0017$ and -0.0014 for the Rodionov, Sather and CTEQ4LQ PDFs, respectively. The CSV corrections decrease the NuTeV discrepancy in the Weinberg angle by about 30%, or one standard deviation. While some groups have obtained substantially smaller estimates for the charge symmetry violating contribution to the NuTeV anomaly [44, 48], in the first case the constraint on baryon number was not respected while the second paper assumed a completely different mechanism for parton CSV. On the other hand, as we discuss next, the phenomenological values for CSV allow considerably larger isospin violation than any of the theoretical estimates.

Valence quark CSV makes a substantially larger contribution than sea quark CSV to the extraction of the Weinberg angle from neutrino DIS. Using the sea-quark CSV and the best-fit value for valence quark CSV obtained by the MRST group, would remove roughly 1/3 of the NuTeV anomaly. The value $\kappa = -0.6$, within the 90% confidence limit found by MRST, would completely remove the NuTeV anomaly, while the value $\kappa = +0.6$ would double the discrepancy. The MRST results show that isospin violating PDFs are able to completely remove the NuTeV anomaly in the Weinberg angle, or to make it twice as large, without serious disagreement with any of the data used to extract quark and gluon PDFs.

There are other possible corrections to the Weinberg angle extracted by the NuTeV experiment, but for the most part the corrections are small and/or well understood. The correction for the neutron excess in iron is large, but apparently well known [43, 44]. Radiative corrections are also large, but also believed to be under control [49], although the radiative corrections are being re-analyzed [50]. The situation with strange quarks is not certain. Spontaneously broken chiral SU(3) $\times$ SU(3) symmetry implies an asymmetry between $s(x)$ and $\bar{s}(x)$ [51]. As a direct consequence of such an asymmetry there is a correction to the extraction of the Weinberg angle that depends on the momentum asymmetry

$$S_{\rm v} = \int_0^1 x\,[s(x) - \bar{s}(x)]\;dx\,. \tag{17}$$

A positive (negative) value for $S_{\rm v}$, meaning that strange quarks carry more (less) net momentum than strange antiquarks, would decrease (increase) the size of the Weinberg anomaly. The strange quark and antiquark distributions can be extracted from the cross sections for opposite sign dimuons in reactions induced by neutrinos or antineutrinos; such reactions have been measured by the CCFR [20] and NuTeV [21] collaborations. The NuTeV group has extracted strange and antistrange PDFs from the dimuon production reactions; they obtain values for $S_{\rm v}$ that are consistent with zero, or perhaps small and negative [44]. The CTEQ group on the other hand [52, 53, 54], has included the dimuon data in

a global fit of PDFs; they obtain positive values for S_v that could account for roughly one-third of the Weinberg angle anomaly. In both NuTeV and CTEQ analyses the strange quark distributions are determined from the same CCFR/NuTeV dimuon data, but at present the two analyses obtain qualitatively different results for the strange quark momentum asymmetry.

In conclusion, it seems that the magnitude of CSV effects allowed by the MRST fit makes charge symmetry violation one of the only viable explanations for the anomalous value of the Weinberg angle obtained in the NuTeV neutrino experiment. If CSV effects are sufficiently large to remove the Weinberg angle anomaly, such effects should be visible in various other experiments. We had previously suggested several experiments that could potentially reveal the presence of parton CSV [5]. However, the magnitude of those effects were based on theoretical calculations that predicted substantially smaller CSV effects than are allowed by MRST. It is clearly of great interest now to investigate this issue experimentally.

Acknowledgments

This work was supported in part [JTL] by National Science Foundation research contract PHY0302248 and by [AWT] DOE contract DE-AC05-84ER40150, under which SURA operates Jefferson Laboratory. The authors wish to thank G.P. Zeller and K. McFarland of the NuTeV collaboration, W. Melnitchouk at JLab, and R.S. Thorne from the MRST group, for useful discussions regarding the issues presented here.

References

[1] G. A. Miller, B. M. K. Nefkens and I. Slaus, Phys. Rep. **194**,1 (1990).
[2] E. M. Henley and G. A. Miller in *Mesons in Nuclei*, eds M. Rho and D. H. Wilkinson (North-Holland, Amsterdam 1979).
[3] A.D. Martin, R.G. Roberts, W.J. Stirling and R.S. Thorne, Rep. IPPP/03/45, arXiv:hep-ph/0308087.
[4] G.P. Zeller, K.S. McFarland, T. Adams, A. Alton, S. Avvakumov, L. de Barbaro, P. de Barbaro, R.H. Bernstein, A. Bodek, T. Bolton, J. Brau, D. Buchholz, H. Budd, L. Bugel, J. Conrad, R.B. Drucker, B.T. Fleming, R. Frey, J.A. Formaggio, J. Goldman, M. Goncharov, D.A. Harris, R.A. Johnson, J.H. Kim, S. Koutsoliotas, M.J. Lamm, W. Marsh, D. Mason, J. McDonald, C. McNulty, D. Naples, P. Nienaber, A. Romosan, W.K. Sakumoto, H. Schellman, M.H. Shaevitz, P. Spentzouris, E.G. Stern, N. Suwonjandee, M. Tzanov, M. Vakili, A. Vaitaitis, U.K. Yang, J. Yu and E.D. Zimmerman, Phys. Rev. Lett. **88**, 091802 (2002).
[5] J. T. Londergan and A. W. Thomas, Prog. Part. Nucl. Phys. **41**, 49 (1998).
[6] CCFR Collaboration, W.G. Seligman *et al.,* , Phys. Rev. Lett. **79**, 1213 (1997).
[7] NMC Collaboration, P. Amaudruz *et al.,* , Phys. Rev. Lett. **66**, 2712 (1991); Phys. Lett. B**295**, 159 (1992).
[8] NMC Collaboration, M. Arneodo *et al.,* , Nucl. Phys. B**483**, 3 (1997).
[9] BCDMS Collaboration, A.C. Benvenuti *et al.,* , Phys. Lett. B**237**, 592 (1990).
[10] BCDMS Collaboration, A.C. Benvenuti *et al.,* , Phys. Lett. B**195**, 91 (1987).
[11] L.C. Whitlow *et al.,* , Phys. Lett. B**282**, 475 (1992).
[12] L.C. Whitlow, Ph.D. thesis, Stanford University, preprint SLAC-357 (1990).
[13] F. M. Steffens, W. Melnitchouk and A. W. Thomas, Eur. Phys. J. C **11**, 673 (1999) [arXiv:hep-ph/9903441].
[14] R.G. Arnold *et al.,* , Phys. Rev. Lett. **52**, 727 (1984).
[15] J. Gomez *et al.,* , Phys. Rev. D**49**,4348 (1994).
[16] New Muon Collaboration, M. Amaudruz *et al.,* , Nucl. Phys. B**441**, 3 (1995).
[17] E665 Collaboration, M. R. Adams *et al.,* , Z. Phys. C**67**, 403 (1995).
[18] W.G. Seligman, Ph.D. thesis, Columbia University; Nevis Reports 292, 1997.
[19] G. A. Miller and A. W. Thomas, arXiv:hep-ex/0204007.
[20] CCFR Collaboration, A.O. Bazarko *et al.,* , Z. Phys. C**65**, 189 (1995).
[21] NuTeV Collaboration, M. Goncharov *et al.,* , Phys. Rev. D**64**, 112006 (2001).
[22] Nuclear effects in neutrino reactions should consist of "shadowing" corrections at small x, "EMC"-type corrections at intermediate x, and Fermi-motion effects at large x. Fermi-motion effects are expected to be identical to those seen in muon DIS; shadowing effects for neutrinos should differ from muon DIS on the same nuclear target, see Ref. [23]; and EMC effects may also differ between muons and neutrinos.
[23] C. Boros, J.T. Londergan and A.W. Thomas, Phys. Rev. D**58**, 114030 (1998).
[24] In the published values of the charge ratio, the discrepancy at small x is even larger than shown here. The calculations shown here included estimates of shadowing for neutrino CC reactions that differed from the shadowing observed in DIS for charged leptons, see Ref. [23].
[25] S.J. Brodsky and B.-Q. Ma, Phys. Lett. B**381**, 317 (1996).
[26] C. Boros, J.T. Londergan and A.W. Thomas, Phys. Rev. Lett. **81**, 4075 (1998).
[27] CCFR Collaboration, U.K. Yang *et al.,* , Phys. Rev. Lett. **86**, 2742 (2001).
[28] H. Georgi and H.D. Politzer, Phys. Rev. D**14**, 1829 (1976); R.M. Barnett, Physica D**14**, 70 (1976).
[29] C. Boros, F.M. Steffens, J.T. Londergan and A.W. Thomas, Phys. Lett. B**468**, 161 (1999).
[30] G. Kramer, B. Lampe and H. Spiesberger, Z. Phys. C**72**, 99 (1996).
[31] R.S. Thorne and R.G. Roberts, Phys. Lett. B**421**, 303 (1998).

[32] M. Aivazis, J. Collins, F. Olness and W.K. Tung, Phys. Rev. D**50**, 3102 (1994).

[33] A. I. Signal and A. W. Thomas, Phys. Rev. D **40** (1989) 2832.

[34] A. W. Schreiber, A. I. Signal and A. W. Thomas, Phys. Rev. D **44** (1991) 2653.

[35] A. I. Signal, A.W. Schreiber and A. W. Thomas, Mod. Phys. Lett. A**6**, 271 (1991).

[36] E. Sather, Phys. Lett. **B274**, 433 (1992).

[37] E. N. Rodionov, A. W. Thomas and J. T. Londergan, Mod. Phys. Lett. A **9**, 1799 (1994).

[38] E605 Collaboration, G. Moreno *et al.,* Phys. Rev. D**43**, 2815 (1991).

[39] When MRST, Ref. [3], carry out the global fits allowing either valence or sea CSV, the best-fit PDFs change slightly from the values obtained when charge symmetry is enforced. In our calculations we have used the modified PDFs supplied to us by R.S. Thorne (private communication).

[40] C.J. Benesh and J. T. Londergan, Phys. Rev. C**58**, 1218 (1998).

[41] E. A. Paschos and L. Wolfenstein, Phys. Rev. **D7**, 91, (1973).

[42] D. Abbaneo *et al.,* , CERN Report CERN-EP/2001-098, arXiv:hep-ex/0112021.

[43] S. Davidson, S. Forte, P. Gambino, N. Rius and A. Strumia, JHEP **0202**, 037 (2002) [arXiv:hep-ph/0112302].

[44] G.P. Zeller, K.S. McFarland, T. Adams, A. Alton, S. Avvakumov, L. de Barbaro, P. de Barbaro, R.H. Bernstein, A. Bodek, T. Bolton, J. Brau, D. Buchholz, H. Budd, L. Bugel, J. Conrad, R.B. Drucker, B.T. Fleming, R. Frey, J.A. Formaggio, J. Goldman, M. Goncharov, D.A. Harris, R.A. Johnson, J.H. Kim, S. Koutsoliotas, M.J. Lamm, W. Marsh, D. Mason, J. McDonald, C. McNulty, D. Naples, P. Nienaber, A. Romosan, W.K. Sakumoto, H. Schellman, M.H. Shaevitz, P. Spentzouris, E.G. Stern, N. Suwonjandee, M. Tzanov, M. Vakili, A. Vaitaitis, U.K. Yang, J. Yu and E.D. Zimmerman, Phys. Rev. **D65**, 111103 (2002).

[45] J. T. Londergan and A. W. Thomas, P. Lett. **B558**, 132 (2003); arXiv:hep-ph/0301147.

[46] J. T. Londergan and A. W. Thomas, Phys. Rev. **D67**, 111901 (2003); arXiv:hep-ph/0303155.

[47] H.L. Lai, J. Huston, S. Kuhlmann, F. Olness, J. Owens, D. Soper, W.K. Tung and H. Weerts, Phys. Rev. **D55**, 1280 (1997).

[48] F. G. Cao and A. I. Signal, P. Lett. **B559**, 229 (2003), arXiv:hep-ph/0302206.

[49] D. Yu. Bardin and V.A. Dokuchaeva, report JINR-E2-86-260, unpublished.

[50] K. McFarland, private communication.

[51] A. I. Signal and A. W. Thomas, Phys. Lett. B **191**, 205 (1987).

[52] S. Kretzer, talk presented at XXXIX Rencontres de Montreal, arXiv:hep-ph/0405221.

[53] F. Olness, J. Pumplin, D. Stump, J. Huston, P. Nadolsky, H.L. Lai, S. Kretzer, J.F. Owens, and W.K. Tung, arXiv:hep-ph/0312323.

[54] S. Kretzer, F. Olness, J. Pumplin, M.H. Reno, D. Stump, and W.K. Tung, arXiv:hep-ph/0312322.